LungNet-CT: A Unified Deep Learning Framework for Efficient Lung Cancer Classification from CT Images

1nd Dhekra BEN SASSI
LARODEC Laboratory, ISG Tunis,
Université de Tunis, Tunisia

2nd Marouene CHAIEB
LARODEC Laboratory, ISG Tunis,
Université de Tunis, Tunisia
ENSI, Manouba University, Tunisia

3nd Abdelfetteh AZZOUZ
ENSI, Manouba University, Tunisia

4rd Mohamed El Hedi DOUDECH
ENSI, Manouba University, Tunisia

5th Wissem FERJANI
ENSI, Manouba University, Tunisia

***Abstract*—Early and accurate detection of Lung Cancer remains a major challenge in medical imaging. This paper investigates deep learning approaches for the classification of lung CT images into three categories: normal, benign, and malignant. Three convolutional neural network architectures are evaluated, namely a custom CNN, MobileNetV2, and Xception. The proposed workflow relies on a two-stage data strategy. The models are first trained on the LIDC-IDRI dataset to learn general lung and nodule-related features, and then fine-tuned on IQ-OTH/NCCD for the target three-class classification task. A unified preprocessing pipeline is applied, including resizing, rescaling, label encoding, batching, and shuffling. Performance is assessed using accuracy, loss, recall, and F1-score, with an additional 5-fold cross-validation experiment to evaluate robustness. The results show that Xception achieved the best predictive performance, with an accuracy of 0.993 and an F1-score of 0.992. MobileNetV2 also delivered strong results, reaching an accuracy of 0.982 and an F1-score of 0.981, while offering lower computational cost. The custom CNN remained competitive, with an accuracy of 0.961 and an F1-score of 0.930. The cross-validation results further supported the effectiveness of the workflow, highlighting a clear performance–efficiency trade-off between the evaluated models. The source code is publicly available on LungNet-CT.**

***Index Terms*—Lung cancer classification, CT imaging, Medical Image Analysis, Computer-Aided Diagnosis (CAD), Convolutional Neural Networks (CNNs), Transfer Learning.**

I. Introduction

Lung Cancer (LC) remains one of the most serious health challenges worldwide, and its prognosis is strongly influenced by the stage at which it is detected. Computed tomography (CT) imaging plays an important role in the identification of pulmonary nodules and suspicious lesions, but manual interpretation can be time-consuming and subject to variability. These challenges have motivated growing interest in automated decision-support systems based on deep learning.

Deep learning models have demonstrated strong performance in medical image analysis because of their ability to learn hierarchical visual features directly from image data. Recent work has shown that architectural refinement and systematic hyperparameter tuning can further improve performance in challenging medical imaging tasks [1]. In the context of lung cancer analysis, recent studies have explored both lightweight and high-capacity architectures, as well as ensemble strategies, to improve diagnostic accuracy. However, the balance between predictive performance and computational practicality remains an important issue, especially for applications that may later need to operate in constrained clinical environments.

Lung cancer classification from CT images has attracted growing interest due to the potential of deep learning to support earlier and more reliable diagnosis. However, the choice of model architecture remains an important issue. While high-capacity deep networks may achieve strong predictive performance, they often require greater computational resources, which can reduce their practical suitability. Conversely, lighter architectures may offer faster and more efficient inference, but their classification performance must still be carefully assessed. This creates a need for controlled evaluations that compare different architectures under a unified workflow rather than under heterogeneous experimental settings.

This paper investigates three deep learning architectures for three-class lung CT classification: a custom CNN, MobileNetV2, and Xception. Rather than proposing a completely new architecture, the objective is to fine-tune and evaluate these models under a unified workflow using a two-stage data strategy based on LIDC-IDRI for initial feature learning and IQ-OTH/NCCD for task-specific fine-tuning.

The main paper contribution is a unified evaluation framework that enables a consistent comparison of the three architectures in terms of predictive performance and computational efficiency. Section II reviews the related work on deep learning for lung cancer classification from CT images and highlights the research gap addressed in this study. Section III describes the proposed methodology, including the datasets, preprocessing pipeline, model architectures, training strategy, and evaluation metrics. Section IV presents the experimental results, while Section V discusses the findings. Finally, Section VI concludes the paper and suggests future research directions.

II. Related Work and Research Gap

Deep learning has become a central approach for lung cancer analysis from medical images, especially for CT-based detection and classification tasks. Recent studies have explored a broad range of methods, including custom CNNs, transfer-learning architectures, ensemble models, and lightweight networks. While many of these approaches report strong predictive performance, they also reveal recurring challenges related to computational complexity, limited external validation, and practical deployment in clinical settings.

Several studies have relied on ensemble or hybrid frameworks to improve predictive performance. Gautam et al. [2] proposed a weighted ensemble combining ResNet-152, DenseNet-169, and EfficientNet-B7 on the LIDC-IDRI dataset, achieving 97.23% accuracy and 98.6% sensitivity. Obayya et al. [3] introduced a hybrid framework integrating GhostNet, an Echo State Network, and Tuna Swarm optimization, and reported 99.33% accuracy. Majumder et al. [4] developed MENet, which combines Xception, InceptionResNetV2, and MobileNetV2 using a fuzzy-ranking mechanism on LIDC-IDRI and IQ-OTH/NCCD. Although these approaches achieve strong results, they often rely on multi-model pipelines that may increase inference cost and reduce practical feasibility.

Other works have focused on custom CNNs and transfer learning for lung cancer classification. Hammad et al. [5] proposed a custom CNN combined with Grad-CAM to improve interpretability, reaching 93.06% accuracy. Mamun et al. [6] introduced a lightweight CNN framework for CT-based diagnosis and compared it with transfer-learning models, reporting 92% accuracy and 91.72% recall. Nishio et al. [7] showed that transfer learning significantly improved a VGG16-based deep CNN for pulmonary nodule classification, although the final accuracy remained lower than more recent approaches. These studies confirm the value of CNN-based models, while also showing that architecture choice has a strong effect on both predictive performance and computational efficiency.

The literature also underlines the importance of data preparation, balancing strategies, and clinically relevant validation. Musthafa et al. [8] applied SMOTE-based balancing on IQ-OTH/NCCD and reported 99.64% accuracy. Pandian et al. [9] combined CNN and GoogleNet with multi-planar CT analysis and achieved 98% precision. Ali et al. [10] integrated an ML-CNN with IoMT data and PSO-based tuning, reaching 98.45% accuracy. In parallel, explainability and deployment issues are receiving increasing attention. Liz-López et al. [11] emphasized that explainable AI remains underused in lung cancer imaging despite its clinical relevance, while Wehbe et al. [12] combined detection and staging in a unified deep learning system with strong precision and real-time inference.

From an applied decision-support perspective, similar challenges have been studied in healthcare operations research. For instance, the integrated recovery room planning and scheduling problem during the COVID-19 pandemic [13] highlights the need for adaptive and constraint-aware optimization strategies under dynamic clinical conditions. This perspective is aligned with the requirements of medical AI systems, where models must efficiently incorporate new information while respecting operational and clinical constraints.

In addition, game-theoretic approaches have been widely explored for modeling competitive and multi-agent decision-making problems. For example, a Stackelberg game-based competitive intelligence framework involving a three-player scenario demonstrates how hierarchical optimization strategies can be used to model interactions between competing agents under strategic constraints [14].

The reviewed literature confirms the strong potential of deep learning for lung cancer analysis from CT images, but it also reveals several recurring limitations. First, many high-performing methods rely on complex or computationally expensive architectures, such as multi-model ensembles or hybrid optimization pipelines, which may reduce their suitability for practical deployment. Second, a large part of the literature focuses on performance on a single benchmark dataset, making it difficult to assess the consistency of reported results across different imaging conditions. Third, although high predictive accuracy is frequently emphasized, fewer studies explicitly examine the trade-off between classification performance and computational efficiency under a unified experimental protocol. These observations motivate the present study, which focuses on the fine-tuning and evaluation of three CNN-based architectures with different computational characteristics—a custom CNN, MobileNetV2, and Xception—for three-class lung CT classification.

III. Methodology

This section describes the methodology adopted for LC classification from CT images. The proposed workflow combines a two-stage data strategy, a unified preprocessing pipeline, and the evaluation of 3 CNN architectures, namely a custom CNN, MobileNetV2, and Xception. The overall process includes data preparation, baseline training, fine-tuning, and validation. Figure 1 presents the overall methodology adopted in this study, highlighting the two-stage workflow based on initial training with LIDC-IDRI, subsequent fine-tuning on IQ-OTH/NCCD, and final evaluation.

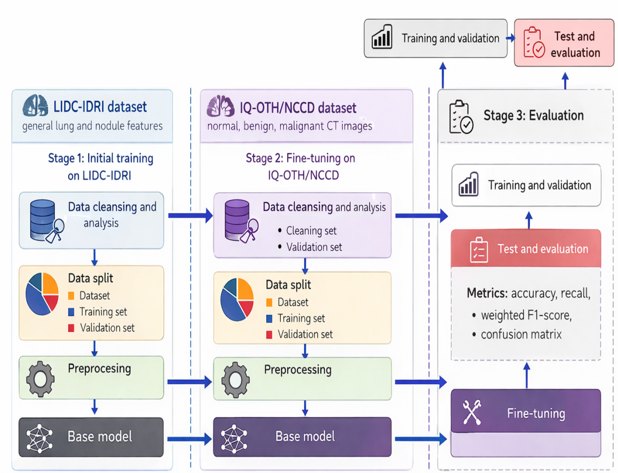

Fig. 1: Overview of the proposed methodology for lung cancer classification

TABLE I: Detailed Summary of Related Work on Lung Cancer Classification

Study / Author	Method	Key Contributions
Gautam et al. (2024) [2]	Weighted ensemble of ResNet-152, DenseNet-169, EfficientNet-B7	CT-based lung nodule severity classification on LIDC-IDRI; reported 97.23% accuracy and 98.6% sensitivity; limited by ensemble complexity and need for broader external validation.
Hammad et al. (2025) [5]	Custom CNN + Grad-CAM	CT-based lung cancer subtype classification with explainability; achieved 93.06% accuracy; improved interpretability through Grad-CAM visualizations.
Ali et al. (2023) [10]	ML-CNN + IoMT + PSO	Integrated CT and IoMT data for early diagnosis; achieved 98.45% accuracy; highlighted efficient diagnosis but depends on sensor data quality.
Obayya et al. (2023) [3]	GhostNet + ESN + Tuna Swarm Algorithm	Hybrid deep learning framework for colon and lung cancer detection; achieved 99.33% accuracy; computationally sophisticated but highly accurate.
Nishio et al. (2020) [7]	VGG16-based DCNN with transfer learning	Compared deep learning and radiomics for pulmonary nodule classification; showed transfer learning improved performance, reaching 68.0% accuracy.
Musthafa et al. (2023) [8]	CNN + SMOTE	Lung cancer stage classification on IQ-OTH/NCCD; reported 99.64% accuracy; highlighted the impact of class balancing on performance.
Mamun et al. (2023) [6]	Lightweight custom CNN	CT-based lung cancer diagnosis using a CNN optimized for efficiency; achieved 92% accuracy and 91.72% recall.
Tsukamoto et al. (2022) [15]	Fine-tuned DCNNs + additional classifiers	Automated classification of lung cancer cytology images; improved classification performance through hybrid deep learning and classical classifiers.
Li et al. (2019) [16]	Faster R-CNN with 3D MRI slices	Early lung nodule detection using thoracic MRI; introduced multi-slice spatial context and achieved 85.2% sensitivity with 3.47 false positives per scan.
Emwal et al. (2024) [17]	Deep CNN models on histopathology images	Automated lung cancer detection from histopathology images; highlighted strong performance of VGG-based models.
Liz-López et al. (2025) [11]	Review of deep learning methods	Reviewed CNNs, 3D CNNs, attention mechanisms, and ensemble models; emphasized challenges related to reproducibility, interpretability, and real-world validation.
Majumder et al. (2024) [4]	MENet ensemble (Xception, InceptionResNetV2, MobileNetV2)	CT-based classification using a fuzzy-ranking ensemble; strong performance on LIDC-IDRI and IQ-OTH/NCCD, but with higher computational complexity.
Pandian et al. (2022) [9]	CNN + GoogleNet	Multi-planar CT analysis for lung cancer detection; achieved 98% precision and emphasized hybrid feature extraction.
Wehbe et al. (2024) [12]	YOLOv8 + TNM-Classifier	Unified deep learning system for lung cancer detection and TNM staging; combined strong precision with real-time inference capability.

A. Dataset Description and Characteristics

Two datasets were used in this study. The first is the LIDC-IDRI dataset, which provides thoracic CT scans with annotated lung nodules and serves as the source of general lung and nodule-related information during the initial training stage. The second is the IQ-OTH/NCCD dataset, which is used for the target three-class classification task involving normal, benign, and malignant CT images. This combination allows the models to benefit from both broad anatomical variability and clinically focused cases.

B. Preprocessing Pipeline

A unified preprocessing pipeline was applied to prepare the CT images for training and evaluation. The images were resized according to the input requirements of each architecture: 244×244 for the custom CNN, 224×224 for MobileNetV2, and 256×256 for Xception. Since the datasets were already pre-augmented, no additional augmentation stage was introduced during training. Pixel intensities were normalized using a rescaling layer that transformed the original range $[0, 255]$ into the interval $[-1, 1]$, which supports stable training and faster convergence. The class labels were then converted into one-hot encoded vectors for the three target classes, and the data were batched and shuffled to improve training efficiency and generalization.

C. Model Architectures

Three CNN architectures were considered in this study. Table II summarizes the main architectural and computational characteristics of the three evaluated models.

TABLE II: Model specifications of the evaluated architectures

Parameter	Custom CNN	MobileNetV2	Xception
Input resolution	$244 \times 244 \times 3$	$224 \times 224 \times 3$	$256 \times 256 \times 3$
Trainable parameters	8.4M	3.5M	22.9M
Total layers	12	54	71
Batch size	32	32	16
Learning rate	1×10^{-4}	1×10^{-4}	5×10^{-5}
Dropout rate	0.3	0.2	0.4
FLOPs	1.2B	0.8B	3.2B
Memory usage	450MB	300MB	1200MB

Custom CNN: The custom CNN was used as a baseline architecture tailored to the target classification task. It consists of stacked convolutional layers with batch normalization and max-pooling, followed by dense layers and dropout regularization for three-class prediction. This architecture was designed to provide a task-specific reference model for comparison with MobileNetV2 and Xception.

MobileNetV2: MobileNetV2 was used as a lightweight transfer-learning architecture for efficient lung CT classification. The model processes inputs of size $224 \times 224 \times 3$ after rescaling, uses a pretrained backbone with `include_top=False`, and keeps the base network frozen during this stage. Feature extraction is followed by global average pooling and a dropout-regularized classification head for three-class prediction.

Xception: Xception was adopted as the most expressive architecture among the evaluated models. In the implemented configuration, the model receives input images of size $256 \times 256 \times 3$ after rescaling. A pretrained Xception backbone was used with `include_top=False`, while the base network remained frozen during this stage. The extracted features were passed through a `GlobalAveragePooling2D` layer, followed by dropout regularization and a dense classification layer with L2 regularization for three-class prediction. This architecture was selected to capture richer and more detailed image representations for distinguishing between normal, benign, and malignant CT patterns.

D. Training Strategy

The training process was organized into three phases.

Phase 1 – Baseline Training: Each model was first trained for 50 epochs using the original training/validation split in order to establish a baseline and verify the selected architectural configuration.

Phase 2 – Fine-Tuning: After baseline training, the models were fine-tuned using augmented CT scans derived from IQ-OTH/NCCD, while validation and testing were performed on real CT scans from IQ-OTH/NCCD and LungHID. This phase was intended to improve adaptation to the target task and to refine class discrimination. Model performance was then evaluated using accuracy, loss, recall, and F1-score.

Phase 3 - Cross-Validation: To further assess robustness and reduce the overfitting risk, a manual 5-fold cross-validation scheme was applied to Xception, selected as the most expressive architecture among evaluated models. Each fold used a fixed validation set, and fine-tuning was performed for 15 epochs per fold starting from baseline checkpoint.

E. Optimization and Training Configuration

Training was performed using the Adam optimizer. The baseline phase used a learning rate of 1×10^{-4}, whereas the fine-tuning phase used a learning rate of 1×10^{-5}. Early stopping based on validation loss was employed to reduce overfitting. A batch size of 32 was used throughout the training and fine-tuning stages. In addition, automatic mixed precision (AMP) was employed where supported in order to improve computational efficiency and reduce memory usage.

IV. Experimental Results

This section presents the experimental results obtained for the three evaluated architectures, namely the custom CNN, MobileNetV2, and Xception. The experiments were conducted on CT images from the IQ-OTH/NCCD and LungHID datasets under a unified training and evaluation setting. Results are first reported without cross-validation, and then complemented by a 5-fold cross-validation analysis.

A. Comparative Performance Without Cross-Validation

The first set of experiments was conducted using a combined dataset of more than 14,000 augmented CT scans from IQ-OTH/NCCD for training, together with 600 real CT scans for validation and 723 real CT scans for testing from IQ-OTH/NCCD and LungHID. Training was performed for 50 epochs with early stopping. Table III summarizes the obtained results.

Among the three models, Xception achieved the best overall performance, with the highest accuracy, the lowest loss, and the highest recall and F1-score. MobileNetV2 also delivered strong results and remained close to Xception across all reported metrics. The custom CNN achieved competitive performance, although it remained below the two transfer-learning-based models.

TABLE III: Performance of the evaluated models without cross-validation

Model	Accuracy	Loss	Recall	F1-score
Custom CNN	0.961	0.120	0.965	0.930
MobileNetV2	0.982	0.045	0.978	0.981
Xception	0.993	0.032	0.991	0.992

B. Cross-Validation Results

To further assess robustness, a 5-fold cross-validation experiment was conducted during fine-tuning. The same combined dataset was used, with training limited to 50 epochs and early stopping. The results are reported in Table IV.

TABLE IV: Model performance across 5-fold cross-validation

Metric	Fold 1	Fold 2	Fold 3	Fold 4	Fold 5	Avg
Accuracy	0.9834	0.8963	0.9350	0.8091	0.8257	0.8899
Loss	0.0995	0.3112	0.2920	0.5214	0.5081	0.3464
Recall	0.9808	0.8561	0.9089	0.7560	0.7981	0.8600
F1-score	0.9637	0.8517	0.8633	0.6672	0.7026	0.8097

The cross-validation results confirm that the proposed workflow maintains strong performance across multiple folds, with an average accuracy of 0.8899 and an average F1-score of 0.8097. At the same time, the variability between folds indicates that performance remains sensitive to data partitioning, which underlines the importance of complementing a single train–test evaluation with a robustness analysis.

C. Performance Evaluation

In addition to the quantitative results reported in Tables III and IV, visual analysis was carried out using training curves and confusion matrices. The accuracy and loss curves illustrate the convergence behavior of each model during training and fine-tuning, whereas the confusion matrices show the class-wise distribution of correct and incorrect predictions on the test set.

Figures 2 and 3 confirm the same ranking observed in the metric tables. The custom CNN converges steadily and provides a reliable baseline, although its confusion matrix shows more classification errors than the two transfer-learning-based models. MobileNetV2 exhibits stable convergence and strong class-wise prediction performance, consistent with its high accuracy and lower computational cost. Xception shows the most stable convergence and the strongest confusion matrix, which is in line with its superior quantitative results.

Overall, the visual evaluation supports the previous comparative analysis: Xception delivers the strongest predictive performance, MobileNetV2 offers a highly competitive and efficient alternative, and the custom CNN remains a useful baseline under the same workflow.

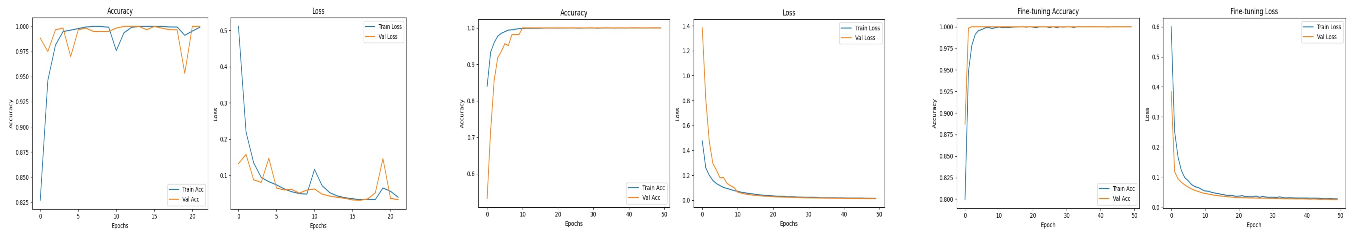

(a) Custom CNN (b) MobileNetV2 (c) Xception

Fig. 2: Training and fine-tuning accuracy/loss curves of the evaluated models. Kindly increase the size of the curves figure

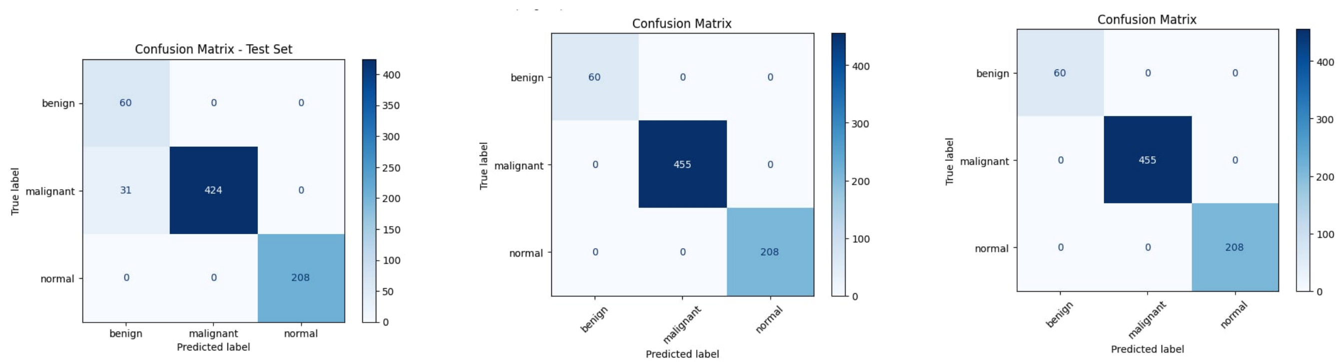

(a) Custom CNN (b) MobileNetV2 (c) Xception

Fig. 3: Confusion matrices of the evaluated models on the test set.

V. Discussion

A. Internal Performance Analysis

The internal comparison confirms the ranking already observed in the results section. Xception achieved the strongest predictive performance, MobileNetV2 remained highly competitive while offering greater efficiency, and the custom CNN served as a reliable but lower-performing baseline.

TABLE V: Final Model Comparison Summary

Criterion	Xception	MobileNetV2	Custom CNN	Best
Test Accuracy	0.993	0.982	0.961	**Xception**
Test Loss	0.032	0.045	0.120	**Xception**
Test Precision	0.993	0.984	0.970	**Xception**
Test Recall	0.991	0.978	0.965	**Xception**
Training Efficiency	Medium	High	Low	**MobileNetV2**
Parameter Count	22.9M	3.5M	8.4M	**MobileNetV2**
Inference Speed	65 ms	22 ms	38 ms	**MobileNetV2**

As shown in Table V, Xception obtained the best values on all major test metrics, whereas MobileNetV2 showed the most favorable efficiency profile, with the lowest parameter count, the fastest inference speed, and the highest training efficiency. This confirms a clear trade-off between predictive performance and computational cost. The cross-validation results reported earlier provide a more cautious view of robustness, since the lower values observed in some folds indicate that performance may vary with data partitioning.

B. Model Stability Across Data Splits

To complement the internal comparison, Table VI reports the train, test, and validation behavior of the three models together with the corresponding performance gaps. This view helps assess the stability of the evaluated architectures across different subsets.

TABLE VI: Performance Comparison of Evaluated Models with Gap Analysis

Model	Data	Loss	Gap (L)	Acc.	Gap (A)	Prec.	Rec.
3*Xception	Train	0.0183	↓1.43	1.00	↑0.06	0.981	0.985
	Test	0.0320	↓8.243	0.993	↑0.11	0.993	0.991
	Valid	0.0276	↓8.24	1.00	↑0.20	0.980	0.976
3*MobileNetV2	Train	0.0127	–	1.00	↑0.09	0.975	0.970
	Test	0.0450	↑0.28	0.982	↑0.10	0.984	0.978
	Valid	0.0133	–	1.00	↑0.45	0.943	0.936
3*Custom CNN	Train	0.0208	↑0.02	0.9998	↑0.00	0.9966	0.9998
	Test	0.1200	↓0.21	0.9610	↑0.04	0.9700	0.9650
	Valid	0.0204	↓0.33	0.9550	↑0.04	1.0000	0.9564

Note: Gap values indicate variation between train, validation, and test performance for each model. ↑ denotes improvement and ↓ denotes degradation.

As shown in Table VI, the three models maintain high train and validation accuracy, but Xception remains the most consistent on the test set, which confirms its stronger generalization within the adopted workflow. MobileNetV2 also shows stable behavior, while the custom CNN exhibits a larger drop in test performance. These observations are consistent with the broader literature, where transfer-learning-based and deeper CNN architectures frequently achieve strong results in lung cancer classification. However, because prior studies use different datasets, label settings, and evaluation protocols, direct numerical comparison remains limited.

C. Summary of Findings

Overall, the discussion confirms that the three architectures are all effective for lung CT classification, but they present different trade-offs. Xception is the strongest model in terms of predictive performance, MobileNetV2 provides the most attractive balance between performance and efficiency, and the custom CNN remains a reliable baseline under the same workflow. Together, Tables V and VI show that the proposed evaluation framework supports both performance comparison and model stability analysis without requiring overly complex architectures.

VI. Conclusion and Future Work

This paper presented a deep learning-based study for lung cancer classification from CT images using three architectures: a custom CNN, MobileNetV2, and Xception. The proposed workflow combined a two-stage data strategy, a unified preprocessing pipeline, and a common evaluation setting, with both direct test performance and 5-fold cross-validation used to assess model behavior.

The results showed that Xception achieved the best predictive performance, reaching an accuracy of 0.993 and an F1-score of 0.992. MobileNetV2 also delivered strong results, with an accuracy of 0.982 and an F1-score of 0.981, while providing a lighter and more efficient architecture. The custom CNN remained competitive as a baseline model, although it performed below the two transfer-learning-based architectures. The cross-validation results further confirmed the effectiveness of the workflow while showing that performance may vary across folds.

Overall, the findings confirm the relevance of convolutional neural networks for automated lung cancer classification from CT images and highlight a clear trade-off between predictive performance and computational efficiency, with Xception favoring accuracy and MobileNetV2 offering a more efficient alternative.

Future work may focus on broader external validation using additional clinical datasets, further assessment of robustness under different imaging conditions, and the integration of efficient models into practical computer-aided diagnostic workflows.

References

[1] M. Chaieb, Y. Hfidhi, D. Ben Sassi, and M. A. Ben Ltaief, "3d-unet+: An enhanced 3d u-net framework for brain tumor segmentation with systematic hyperparameter tuning," *Neural Computing and Applications*, vol. 38, no. 10, p. 389, 2026.

[2] N. Gautam, A. Basu, and R. Sarkar, "Lung cancer detection from thoracic ct scans using an ensemble of deep learning models," *Neural Computing and Applications*, vol. 36, pp. 2459–2477, 2024.

[3] M. Obayya, M. A. Arasi, N. Alruwais, R. Alsini, A. Mohamed, and I. Yaseen, "Biomedical image analysis for colon and lung cancer detection using tuna swarm algorithm with deep learning model," *IEEE Access*, vol. 11, pp. 94 705–94 712, 2023.

[4] S. Majumder, N. Gautam, A. Basu, A. Sau, Z. W. Geem, and R. Sarkar, "Menet: A mitscherlich function based ensemble of cnn models to classify lung cancer using ct scans," *PLOS ONE*, vol. 19, no. 3, p. e0298527, 2024.

[5] M. Hammad, M. ElAffendi, A. A. A. El-Latif, A. A. Ateya, G. Ali, and P. Pławiak, "Explainable ai for lung cancer detection via a custom cnn on ct images," *Scientific Reports*, vol. 15, no. 1, p. 12707, 2025.

[6] M. Mamun, M. I. Mahmud, M. Meherin, and A. Abdelgawad, "Lcd-ctcnn: Lung cancer diagnosis of ct scan images using cnn based model," *Preprint*, 2023.

[7] M. Nishio, O. Sugiyama, M. Yakami, S. Ueno, T. Kubo, T. Kuroda, and K. Togashi, "Computer-aided diagnosis of lung nodule classification between benign, primary lung cancer, and metastatic lung cancer using deep convolutional neural network with transfer learning," *PLOS ONE*, vol. 15, no. 6, p. e0236471, 2020.

[8] M. M. Musthafa, I. Manimozhi, T. R. Mahesh, and S. Guluwadi, "High-accuracy lung cancer stage classification using cnn and smote on ct scans: A machine learning approach for early diagnosis," *Artificial Intelligence in Medicine*, 2023.

[9] R. Pandian, V. Vedanarayanan, D. N. S. R. Kumar, and R. Rajakumar, "Detection and classification of lung cancer using cnn and googlenet," *Measurement: Sensors*, vol. 24, p. 100588, 2022.

[10] Y. H. Ali, V. S. Chooralli, K. Balasubramanian *et al.*, "Optimization system based on convolutional neural network and internet of medical things for early diagnosis of lung cancer," *Bioengineering*, vol. 10, no. 3, p. 320, 2023.

[11] H. Liz-López, Á. A. de Sojo-Hernández, S. D'Antonio-Maceiras *et al.*, "Deep learning innovations in the detection of lung cancer: Advances, trends, and open challenges," *Cognitive Computation*, vol. 17, no. 67, 2025.

[12] A. Wehbe, S. Dellepiane, and I. Minetti, "Enhanced lung cancer detection and tnm staging using yolov8 and tnmclassifier: An integrated deep learning approach for ct imaging," *IEEE Access*, vol. 12, pp. 12 345–12 356, 2024.

[13] M. Chaieb, D. B. Sassi, J. Jemai, and K. Mellouli, "Challenges and solutions for the integrated recovery room planning and scheduling problem during covid-19 pandemic," *Medical & Biological Engineering & Computing*, vol. 60, no. 5, pp. 1295–1311, 2022.

[14] D. B. Sassi and M. Chaieb, "A game theory competitive intelligence solution stimulated from a stackelberg game: A three players scenario," *Engineering Applications of Artificial Intelligence*, vol. 135, p. 108825, 2024.

[15] T. Tsukamoto, A. Teramoto, A. Yamada, Y. Kiriyama, E. Sakurai, A. Michiba, K. Imaizumi, and H. Fujita, "Comparison of fine-tuned deep convolutional neural networks for the automated classification of lung cancer cytology images with integration of additional classifiers," *Asian Pacific Journal of Cancer Prevention*, vol. 23, no. 4, pp. 1315–1324, 2022.

[16] Y. Li, L. Zhang, H. Chen, and N. Yang, "Lung nodule detection with deep learning in 3d thoracic mr images," *IEEE Access*, vol. 7, pp. 37 822–37 832, 2019.

[17] P. Emwal, R. Saini, S. Singh, and M. Mittal, "Lung cancer detection using deep-learning models," in *Soft Computing and Its Engineering Applications (icSoftComp 2024)*, 2024.